Physicochemical Properties and Structures of Room Temperature Ionic Liquids. 2. Variation of Alkyl Chain Length in Imidazolium Cation

Hiroyuki Tokuda,[†] Kikuko Hayamizu,[‡] Kunikazu Ishii,[†] Md. Abu Bin Hasan Susan,[†,§] and Masayoshi Watanabe*[,†]

Department of Chemistry and Biotechnology, Yokohama National University, and CREST-JST, 79-5 Tokiwadai, Hodogaya-ku, Yokohama 240-8501, Japan, and National Institute of Advanced Industrial Science and Technology, AIST Tsukuba Centre 5, Tsukuba 305-8565, Japan

Received: November 25, 2004; In Final Form: January 14, 2005

The alkyl chain length of 1-alkyl-3-methylimidazolium bis(trifluoromethane sulfonyl)imide ([Rmim][$(CF_3SO_2)_2N$], R = methyl (m), ethyl (e), butyl (b), hexyl (C_6), and octyl (C_8)) was varied to prepare a series of room-temperature ionic liquids (RTILs), and the thermal behavior, density, viscosity, self-diffusion coefficients of the cation and anion, and ionic conductivity were measured over a wide temperature range. The self-diffusion coefficient, viscosity, ionic conductivity, and molar conductivity change with temperature following the Vogel−Fulcher−Tamman equation, and the density shows a linear decrease. The pulsed-field-gradient spin−echo NMR method reveals a higher self-diffusion coefficient for the cation compared to that for the anion over a wide temperature range, even if the cationic radius is larger than that of the anion. The summation of the cationic and anionic diffusion coefficients for the RTILs follows the order [emim][$(CF_3SO_2)_2N$] > [mmim][$(CF_3SO_2)_2N$] > [bmim][$(CF_3SO_2)_2N$] > [C_6mim][$(CF_3SO_2)_2N$] > [C_8mim][$(CF_3SO_2)_2N$], which greatly contrasts to the viscosity data. The ratio of molar conductivity obtained from impedance measurements to that calculated by the ionic diffusivity using the Nernst−Einstein equation quantifies the active ions contributing to ionic conduction in the diffusion components, in other words, ionicity of the ionic liquids. The ratio decreases with increasing number of carbon atoms in the alkyl chain. Finally, a balance between the electrostatic and induction forces has been discussed in terms of the main contribution factor in determining the physicochemical properties.

Introduction

The great interest in room temperature ionic liquids (RTILs) has recently rendered them one of the most attractive materials.[1,2] Since RTILs are comprised entirely of ions, physicochemical properties, as generally characterized by nonvolatility, nonflammability, chemical and thermal stability, and high ionic-conductivity, can be easily tuned simply by changing the structure of the component ions. For practical use in diverse applications, the molecular design of the RTILs has, therefore, been the most fascinating domain of the current research.

Numerous attempts to gain the fundamental understanding of the unique characteristics of the RTILs include combinations of new anions and cations to prepare novel ionic liquids, and studies on their physical properties such as thermal behavior, density, viscosity, and ionic conductivity, as well as on chemical properties, such as solubility of liquids and gases, and polarity.[3−27] However, microscopic information about the ionic state and ion dynamics, which directly influence physicochemical properties of the ionic liquids, has been scarce. Furthermore, comprehensive understanding of the general aspects of properties and their correlation with the structures of the RTILs requires a thorough systematic investigation of a wide variety of ionic liquids by changing the cationic and anionic structures.

To accomplish the objective, we have successfully applied the pulsed-field-gradient spin−echo (PGSE) NMR method for the determination of the cationic and anionic self-diffusion coefficients of certain RTILs of 1-methyl-3-ethylimidazolium ([emim]) and 1-butylpyridinium ([bpy]) cations with [BF_4] and [$(CF_3SO_2)_2N$] anions.[28] Recently, we have also demonstrated the effect of the anionic species on physicochemical properties of a series of RTILs with a fixed cation, 1-butyl-3-methylimidazolium ([bmim]), with different anions, [$(C_2F_5SO_2)_2N$], [$(CF_3SO_2)_2N$], [CF_3SO_3], [PF_6], [CF_3CO_2], and [BF_4], as well as the effect of cationic structures with a fixed anion, [$(CF_3SO_2)_2N$] with different caions, [bmim], [bpy], *N*-butyl-*N*-methylpyrrolidinium, and *N*-butyl-*N*,*N*,*N*,-trimethylammonium.[29] By analyzing the physicochemical properties, we have been able to envisage a broad picture of the structural effects on the diffusion mechanism and ion transport behavior. It is also important to note that typical RTILs have alkyl group(s) attached to the cationic structures. To facilitate molecular design of RTILs, fundamental understanding of the effect of the alkyl groups on the microscopic ion dynamics seems to be essential. Although a change in the alkyl chain length has been reported to cause changes in the melting point and other physicochemical properties, including viscosity, density, conductivity, and lipophilicity,[3−5,11−13,20] correlation of the alkyl chain length and the physicochemical properties of RTILs with fixed anionic species still needs to be explored.

In this study, we prepared a series of RTILs with a fixed cationic backbone and anionic structure with a variety of alkyl

[†] Yokohama National University.
[‡] National Institute of Advanced Industrial Science and Technology.
[§] Permanent address: Department of Chemistry, University of Dhaka, Dhaka 1000, Bangladesh.
* To whom correspondence should be addressed: E-mail: mwatanab@ynu.ac.jp. Fax: +81-45-339-3955.

10.1021/jp044626d CCC: $30.25
Published on Web 03/12/2005

chain lengths, i.e., 1-alkyl-3-methylimidazolium bis(trifluoromethane sulfonyl)imide ([Rmim][$(CF_3SO_2)_2N$], R = methyl (m), ethyl (e), butyl (b), hexyl (C_6), and octyl (C_8)). The physicochemical properties have been investigated, focusing on the ion transport properties depending on the change in the alkyl chain length, to know the relationships between the ionic diffusivity, viscosity, and molar conductivity.

Experimental Section

Synthesis. In general, the syntheses of all the RTILs in this study were based on a metathesis reaction of freshly prepared halide salts of the imidazolium cation with different alkyl chain length and $LiN(SO_2CF_3)_2$, following a slight modification of the procedure reported earlier.[22a] The preparation of [emim][$(CF_3SO_2)_2N$] and [bmim][$(CF_3SO_2)_2N$] has been reported in detail in our previous publications.[28,29a] The halide salt, [mmim][I], was prepared by reacting 1-methylimidazole with methyl iodide in cyclohexane under N_2 atmosphere, and the product was purified by recrystallization from 2-propanol/ethyl acetate to yield a white crystalline solid. The [C_6mim][Br] and [C_8mim][Br] were prepared by the quaternization of 1-methylimidazole with the corresponding alkyl bromide under N_2 atmosphere. The resulting products were repeatedly washed with ethyl acetate, and finally dried to remove any volatile solvents under high vacuum. The anion exchange reaction was carried out by adding 1.2 equiv of $LiN(SO_2CF_3)_2$ in water. The [mmim][$(CF_3SO_2)_2N$] was repeatedly washed with water, followed by recrystallization from methanol in a freezer at −20 °C. In the cases of the relatively viscous [C_6mim] and [C_8mim] based ionic liquids, dichloromethane was added to the crude products, and then the organic solutions were extracted several times with water. All of the ionic liquids were finally dehydrated under high vacuum with heating over 48 h, and structures were identified by ^1H and ^{13}C NMR and fast atom bombardment mass spectra.

Water content of all of the RTILs, determined by Karl-Fisher titration, was below 10 ppm. Due to the immiscibility of the RTILs with water, halide content could not be quantitatively determined. However, halide in the aqueous phase in contact with the ionic liquids could not be detected by using an $AgNO_3$ aqueous solution, which indicates very low content of halide-based impurities, if any, in the RTILs. The RTILs were stored and handled in an argon atmosphere glovebox (VAC, $[O_2] < 1$ ppm, $[H_2O] < 1$ ppm).

Measurements. The measurements conducted for the thermal behavior, self-diffusion coefficients, density, viscosity, and ionic conductivity for the RTILs in this study, were similar to those of our previous reports.[29a] The experimental conditions and the techniques used are briefly described here.

Differential scanning calorimetry (DSC) was carried out on a Seiko Instruments DSC 220C under a nitrogen atmosphere with samples hermetically sealed in Al pans and heated to 80 °C followed by cooling to −150 °C and then reheating, unless otherwise noted, at a cooling and heating rate of 10 °C min^{-1}. The glass transition temperature (T_g) and the melting point (T_m) were determined from the DSC thermograms during the programmed reheating steps.

Thermogravimetric measurements were conducted on a Seiko Instruments thermogravimetry/differential thermal analyzer (TG-DTA 6200) with the samples placed in an open aluminum pan and heated from room temperature to 550 °C at a heating rate of 10 °C min^{-1} under a nitrogen atmosphere.

The density measurement was performed with a thermoregulated density/specific gravity meter DA-100 (Kyoto Electronics Manufacturing Co. Ltd) in the range of 15 to 40 °C.

TABLE 1: Thermal Properties of Room Temperature Ionic Liquids

	T_g/ °C[a]	T_m/ °C[a]	ΔH_m/ kJ mol^{-1} [a]	ΔS_m/ J K^{-1} mol^{-1} [b]	T_d/ °C[c]
[mmim][$(CF_3SO_2)_2N$]		26	24.5	81.7	444
[emim][$(CF_3SO_2)_2N$]	−87[d]	−18	24.8	97.1	439
[bmim][$(CF_3SO_2)_2N$]	−87	−3	20.9	77.3	427
[C_6mim][$(CF_3SO_2)_2N$]	−81	−6	4.6	17.3	428
[C_8mim][$(CF_3SO_2)_2N$]	−80				425

[a] Onset temperatures of a heat capacity change (T_g), an endothermic peak (T_m), and an enthalpy of the melting (ΔH_m) determined by differential scanning calrimetry. [b] Entropy of the melting calculated by $\Delta H_m/T_m$. [c] Onset temperatures of mass loss determined by thermogravimetry. [d] Detected by rapid cooling.

The PGSE-NMR measurements were conducted by using a JEOL JNM-AL 400 spectrometer with a 9.4 T narrow bore superconducting magnet equipped with a JEOL pulse field gradient probe and a current amplifier. The self-diffusion coefficients were measured using the simple Hahn spin−echo sequence, incorporating a sine gradient pulse in each τ period. The interval between two gradient pulses, Δ, was set at 50 ms, and the duration of the field gradient, δ, was varied. The samples were inserted into a 5-mm (o.d.) NMR microtube (BMS-005J, Shigemi, Tokyo) and the measurements for the cationic and anionic self-diffusion coefficients in each RTILs were made by using ^1H (399.7 MHz) and ^{19}F (376.1 MHz) nuclei, respectively, at controlled temperatures with gradual cooling from 80 to −10 °C.

The viscosity measurement was carried out with a Toki RE80 cone-plate viscometer under a nitrogen atmosphere at controlled temperature in the range of 80−10 °C.

The bulk ionic conductivity was measured by complex impedance measurements, using a computer-controlled Hewlett-Packard 4192A LF impedance analyzer over the frequency range from 5 Hz to 13 MHz. The measurement of the samples was carried out in a commercially available conductivity cell with platinized platinum electrode cells (TOA Electronics, CG-511B) at controlled temperatures with cooling from 100 to −10 °C.

Results

Thermal Property, Density, and Molar Concentration. Thermal properties of the RTILs, studied by DSC and TG-DTA measurements, are summarized in Table 1. During the reheating step in the DSC thermograms at a scanning rate of 10 °C min^{-1}, [Rmim][$(CF_3SO_2)_2N$] (R = b, C_6, and C_8) ionic liquids exhibit a heat capacity change corresponding to the T_g. At a scanning rate of 50 °C min^{-1}, supercooling state could also be recognized for [emim][$(CF_3SO_2)_2N$], and the T_g could be determined. However, [mmim][$(CF_3SO_2)_2N$] showed no heat capacity change for the glass transition even upon further rapid cooling, due to its relatively rapid crystallization rate compared to other RTILs. An endothermic peak, corresponding to the T_m, was observed for all of the RTILs prepared in this study in the cycle of the measurements except for [C_8mim][$(CF_3SO_2)_2N$], and therefore, the enthalpy and entropy changes for melting (ΔH_m and ΔS_m, respectively) are also listed in Table 1. The behavior of the change in the T_g and T_m with change in the alkyl chain length of the imidazolium cation is rather complicated. Especially, the T_m of [emim][$(CF_3SO_2)_2N$] is quite low. At a scanning rate of 10 °C min^{-1}, [mmim][$(CF_3SO_2)_2N$] and [emim][$(CF_3SO_2)_2N$] do not show T_g and show only T_m, whereas [bmim][$(CF_3SO_2)_2N$] and [C_6mim][$(CF_3SO_2)_2N$] show both T_g and T_m, indicating the relatively slow crystallization kinetics. Thus, the ΔH_m and ΔS_m of the [bmim][$(CF_3SO_2)_2N$] and [C_6mim][(CF_3-

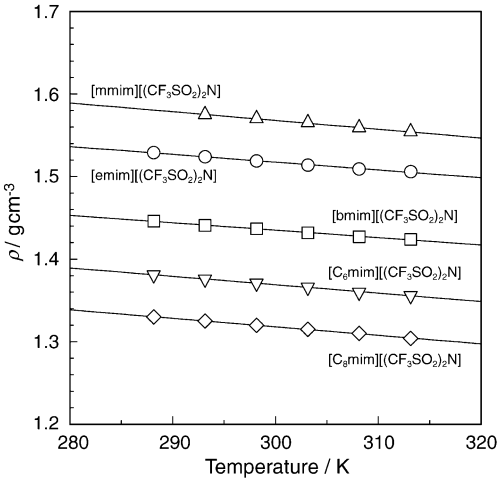

Figure 1. Density of [Rmim][$(CF_3SO_2)_2N$] ionic liquids as a function of temperature.

TABLE 2: Molecular Weight, Density Equation Parameters, and Molar Concentration at 30 °C

$$\rho = b - aT$$

	MW	$a/10^{-3}$ g cm^{-3} K^{-1}	b/ g cm^{-3}	$R^2/10^{-1}$	$M_{30}/10^{-3}$ mol cm^{-3}
[mmim][$(CF_3SO_2)_2N$]	377.3	1.06	1.87	9.99	4.15
[emim][$(CF_3SO_2)_2N$]	391.3	1.00	1.82	10.0	3.87
[bmim][$(CF_3SO_2)_2N$]	419.4	0.94	1.72	9.99	3.42
[C_6mim][$(CF_3SO_2)_2N$]	447.4	1.02	1.67	9.98	3.05
[C_8mim][$(CF_3SO_2)_2N$]	475.5	1.00	1.62	10.0	2.77

$SO_2)_2N$] are only apparent values, because of the coexistence of the crystalline and glassy phase in the cooled samples. On the contrary, we can make a direct comparison for the ΔH_m and ΔS_m between [mmim][$(CF_3SO_2)_2N$] and [emim][$(CF_3SO_2)_2N$]. The reason for the lower T_m for [emim][$(CF_3SO_2)_2N$] can be attributed to a larger entropy gain during the melting transition, since the ΔH_m of [mmim][$(CF_3SO_2)_2N$] and [emim][$(CF_3SO_2)_2N$] are close together. The ethyl group of [emim] has freedom of bond rotation in the liquid state, which may contribute to the larger ΔS_m.

Thermogravimetric results (Table 1) exhibit excellent short-term thermal stability up to 400 °C at a scanning rate of 10 °C min^{-1}. The onset temperatures of mass loss (T_d) decrease with increasing number of carbon atoms in the alkyl chain from [mmim] to [bmim], after which no noticeable change in the T_d can be seen. The thermal stability, in the present case, may be explained by the difference in inductive effects of each hydrocarbon chain attached to the N atom, if the pyrolysis proceeds via an S_N1 reaction. This contrasts with the pyrolysis of the imidazolium salts with different anions, which has been reported to proceed most likely via an S_N2 process, depending on the basicity and/or nucleophilicity of the anions.[19] However, the present observations are in agreement with the finding that thermal stability of the imidazolium-based ionic liquids is affected by the type of isomeric structures of the alkyl groups, as has been evidenced by higher values of the T_d for 1-butyl-2,3-dimethylimidazolium salts than that for 1,2-dimethyl-3-isopropylimidazolium salts, for which the pyrolysis has been presumed to proceed via an S_N1 reaction.[19]

Figure 1 shows the temperature dependency of density for the RTILs, and the density has been found to decrease linearly with increasing temperature. Table 2 lists the best linear-fitting parameters for the density−temperature profiles. The molar concentration (M) calculated from the molecular weight and density of the RTILs at 30 °C is also shown in Table 2. The molar concentration ranges from 2.77 to 4.15 mol L^{-1}. A decrease in the density and an increase in the formula weight with increasing number of carbon atoms in the alkyl chain causes a subsequent decrease in the salt concentration.

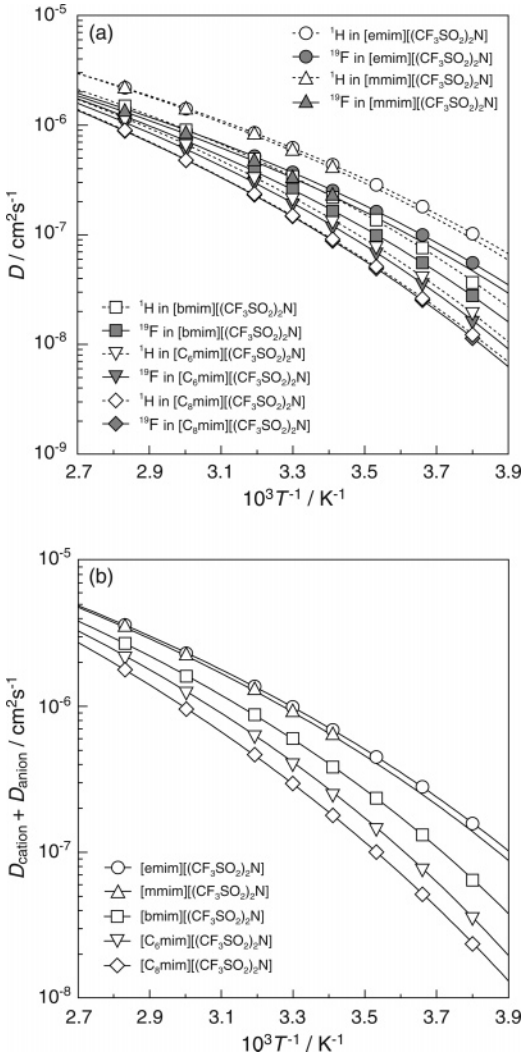

Figure 2. Temperature dependence of (a) self-diffusion coefficients of the cation and anion and (b) simple summation of the cationic and anionic self-diffusion coefficients ($D_{cation} + D_{anion}$) for [Rmim][$(CF_3SO_2)_2N$] ionic liquids.

Ionic Self-Diffusion Coefficient and Viscosity. Figure 2a depicts the temperature dependency of self-diffusion coefficients of the cation (D_{cation}) and anion (D_{anion}) for the [Rmim][$(CF_3SO_2)_2N$] ionic liquids. The simple summation of the cationic and anionic self-diffusion coefficients ($D_{cation} + D_{anion}$) for these RTILs is also shown in Figure 2b. The self-diffusion coefficients as a function of the measuring time (Δ) in the range from 20 to 100 ms did not show any notable dependency for [emim][$(CF_3SO_2)_2N$] and [bmim][$(CF_3SO_2)_2N$], which suggests that the ion diffusion is the Fickian diffusion in the homogeneous fluid. The temperature dependency of the diffusion coefficients in each case exhibits convex curved profiles; therefore, the experimental data have been fitted with the Vogel−Fulcher−Tamman (VFT) equation[30] for diffusivity

$$D = D_0 \exp[-B/(T - T_0)] \quad (1)$$

where the constants D_0 (cm^2 s^{-1}), B (K), and T_0 (K) are adjustable parameters. Table 3 summarizes the best-fit parameters of the ionic diffusivity. The curves calculated by using

TABLE 3: VFT Equation Parameters of Self-Diffusion Coefficient Data

$D = D_0 \exp[-B/(T - T_0)]$			
	$D_0/10^{-4}$ cm^2 s^{-1}	$B/10^2$ K	T_0/K
	[mmim][$(CF_3SO_2)_2$N]		
cation	1.3 ± 0.4	8.47 ± 1.19	146 ± 12
anion	1.0 ± 0.4	9.03 ± 1.30	146 ± 13
cation + anion	2.3 ± 0.7	8.68 ± 1.04	146 ± 11
	[emim][$(CF_3SO_2)_2$N]		
cation	1.1 ± 0.1	8.16 ± 0.41	147 ± 4
anion	0.9 ± 0.1	8.57 ± 0.30	147 ± 3
cation + anion	2.1 ± 0.2	8.36 ± 0.35	146 ± 3
	[bmim][$(CF_3SO_2)_2$N]		
cation	1.1 ± 0.1	8.45 ± 0.37	157 ± 3
anion	1.3 ± 0.3	9.33 ± 0.67	152 ± 6
cation + anion	2.3 ± 0.3	8.84 ± 0.45	155 ± 4
	[C_6mim][$(CF_3SO_2)_2$N]		
cation	1.5 ± 0.2	9.65 ± 0.49	156 ± 4
anion	1.7 ± 0.2	10.10 ± 0.46	154 ± 4
cation + anion	3.2 ± 0.4	9.86 ± 0.35	155 ± 3
	[C_8mim][$(CF_3SO_2)_2$N]		
cation	3.1 ± 0.8	12.46 ± 0.86	140 ± 6
anion	2.5 ± 0.4	11.67 ± 0.56	146 ± 4
cation + anion	5.6 ± 1.1	12.07 ± 0.69	143 ± 5

the best-fit parameters and eq 1 are shown as dashed and solid lines in Figure 2. The summation of the cationic and anionic diffusion coefficients for the ionic liquids follows the order [emim][$(CF_3SO_2)_2$N] > [mmim][$(CF_3SO_2)_2$N] > [bmim][$(CF_3SO_2)_2$N] > [C_6mim][$(CF_3SO_2)_2$N] > [C_8mim][$(CF_3SO_2)_2$N] in the temperature range of the measurements. Although both of the parameters, B and T_0, change with a change in the cationic structure, the change is more pronounced for the B, as compared to the T_0, for each RTIL, which agrees well with our past observations.[29]

Figure 3 shows the temperature dependency of the viscosity (η) for the RTILs. The corresponding VFT equation is

$$\eta = \eta_0 \exp[B/(T - T_0)] \tag{2}$$

where η_0 (mPas), B (K), and T_0 (K) are constants. The best-fit parameters for viscosity are tabulated in Table 4, and the profiles fitted to the VFT equation are represented by solid lines in Figure 3. The macroscopic viscosity values follow the order [C_8mim][$(CF_3SO_2)_2$N] > [C_6mim][$(CF_3SO_2)_2$N] > [bmim][$(CF_3SO_2)_2$N] > [mmim][$(CF_3SO_2)_2$N] > [emim][$(CF_3SO_2)_2$N]

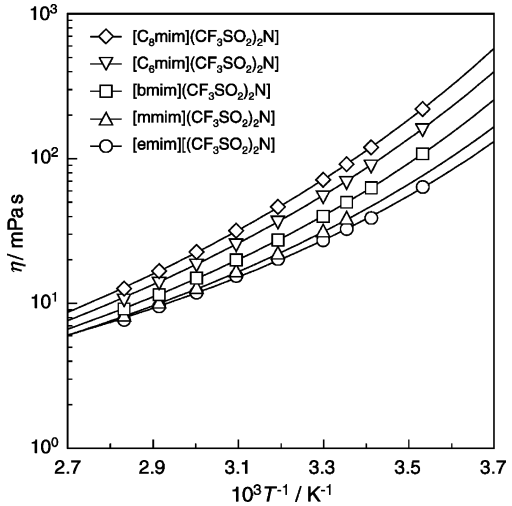

Figure 3. Viscosities of [Rmim][$(CF_3SO_2)_2$N] ionic liquids as a function of temperature.

TABLE 4: VFT Equation Parameters of Viscosity Data

$\eta = \eta_0 \exp[B/(T - T_0)]$			
	$\eta_0/10^{-1}$ mPas	$B/10^{-2}$ K	T_0/K
[mmim][$(CF_3SO_2)_2$N]	2.9 ± 0.6	5.87 ± 0.57	178 ± 7
[emim][$(CF_3SO_2)_2$N]	4.0 ± 1.3	5.09 ± 0.81	182 ± 10
[bmim][$(CF_3SO_2)_2$N]	2.5 ± 0.2	6.25 ± 0.22	180 ± 2
[C_6mim][$(CF_3SO_2)_2$N]	1.6 ± 0.2	7.57 ± 0.39	173 ± 3
[C_8mim][$(CF_3SO_2)_2$N]	1.5 ± 0.2	8.02 ± 0.30	173 ± 2

TABLE 5: VFT Equation Parameters of Ionic Conductivity Data

$\sigma = \sigma_0 \exp[-B/(T - T_0)]$			
	$\sigma_0/10^{-1}$ S cm^{-1}	$B/10^{-2}$ K	T_0/K
[mmim][$(CF_3SO_2)_2$N]	6.6 ± 0.4	5.62 ± 0.18	168 ± 3
[emim][$(CF_3SO_2)_2$N]	5.8 ± 0.2	5.54 ± 0.13	165 ± 2
[bmim][$(CF_3SO_2)_2$N]	4.3 ± 0.2	5.65 ± 0.14	178 ± 2
[C_6mim][$(CF_3SO_2)_2$N]	6.1 ± 0.3	7.31 ± 0.13	168 ± 1
[C_8mim][$(CF_3SO_2)_2$N]	6.1 ± 0.2	8.11 ± 0.12	166 ± 1

in the temperature range of measurements, which greatly contrasts with that of the ionic self-diffusivity (vide infra).

Conductivity. Figure 4 illustrates the temperature dependency of ionic conductivity (σ) for the RTILs in this study. The VFT equation for conductivity is

$$\sigma = \sigma_0 \exp[-B/(T - T_0)] \tag{3}$$

where σ_0 (S cm^{-1}), B (K), and T_0 (K) are constants. Table 5 tabulates the best-fit parameters for conductivity. The high ionic conductivity value of up to 10^{-2} S cm^{-1} for [mmim][$(CF_3SO_2)_2$N], despite lower ionic diffusion coefficients and higher viscosity than that of [emim]-based liquids, can be ascribed to its high molar concentration. Figure 5a exhibits the temperature dependency of the molar conductivity. The VFT equation for the molar conductivity is

$$\Lambda = \Lambda_0 \exp[-B/(T - T_0)] \tag{4}$$

where Λ_0 (S cm^2 mol^{-1}), B (K), and T_0 (K) are constants. Table 6 lists the best-fit parameters for molar conductivity. The molar conductivity of the RTILs can also be calculated from the self-diffusion coefficients (Λ_{NMR}), determined by the PGSE-NMR

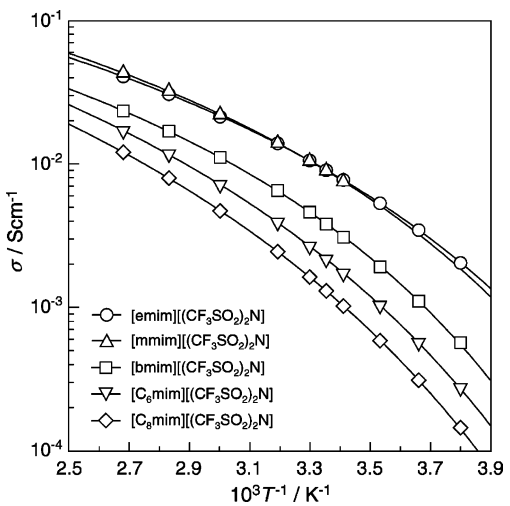

Figure 4. Temperature dependence of ionic conductivity for [Rmim][$(CF_3SO_2)_2$N] ionic liquids.

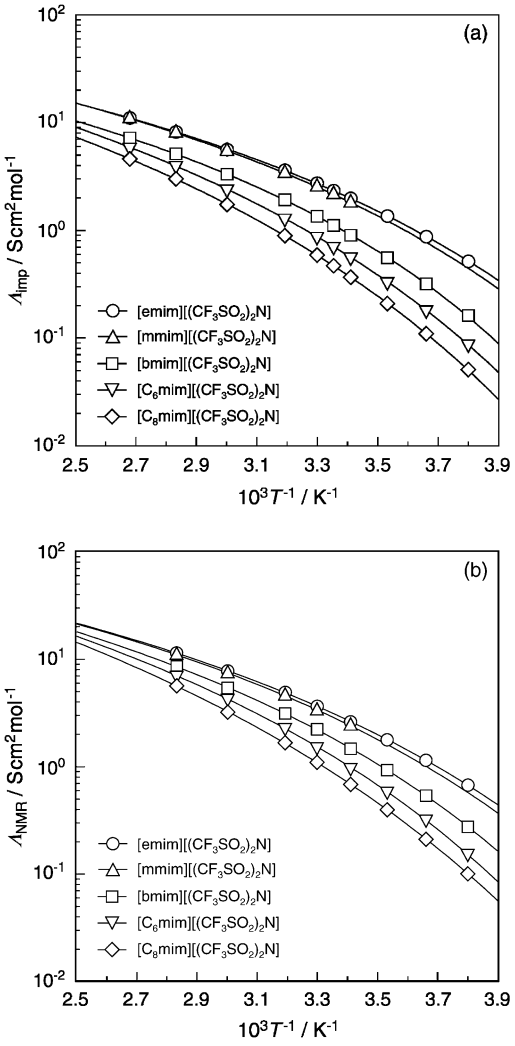

Figure 5. Molar conductivity of [Rmim][$(CF_3SO_2)_2$N] ionic liquids: (a) obtained from ionic conductivity and molar concentration and (b) calculated from ionic self-diffusion coefficients and the Nernst−Einstein equation.

TABLE 6: VFT Equation Parameters of Molar Conductivity Data

	$\Lambda_0/10^2$ S cm^2 mol^{-1}	$B/10^{-2}$ K	T_0/K
$\Lambda_{imp} = \Lambda_0 \exp[-B/(T - T_0)]$			
[mmim][$(CF_3SO_2)_2$N]	2.1 ± 0.1	6.25 ± 0.20	162 ± 3
[emim][$(CF_3SO_2)_2$N]	1.9 ± 0.1	6.04 ± 0.15	161 ± 2
[bmim][$(CF_3SO_2)_2$N]	1.5 ± 0.1	6.05 ± 0.13	175 ± 1
[C$_6$mim][$(CF_3SO_2)_2$N]	2.5 ± 0.1	7.84 ± 0.12	165 ± 1
[C$_8$mim][$(CF_3SO_2)_2$N]	2.8 ± 0.1	8.68 ± 0.12	163 ± 1
$\Lambda_{NMR} = \Lambda_0 \exp[-B/(T - T_0)]$			
[mmim][$(CF_3SO_2)_2$N]	3.2 ± 0.8	6.52 ± 0.82	160 ± 10
[emim][$(CF_3SO_2)_2$N]	3.1 ± 0.3	6.41 ± 0.25	159 ± 3
[bmim][$(CF_3SO_2)_2$N]	3.6 ± 0.4	7.03 ± 0.33	165 ± 3
[C$_6$mim][$(CF_3SO_2)_2$N]	5.0 ± 0.5	8.09 ± 0.33	163 ± 3
[C$_8$mim][$(CF_3SO_2)_2$N]	7.9 ± 1.3	9.90 ± 0.52	153 ± 4

measurements, using the Nernst−Einstein equation

$$\Lambda_{NMR} = N_A e^2 (D_{cation} + D_{anion})/kT = F^2 (D_{cation} + D_{anion})/RT \quad (5)$$

where N_A is the Avogadro number, e is the electric charge on each ionic carrier, k in the Boltzmann constant, F is the Faraday constant, and R is the gas constant. Figure 5b shows the temperature dependency of the molar conductivity calculated from the ionic diffusion coefficient and eq 5, and Table 6 lists the best-fit parameters of the VFT equation. The calculated molar conductivity (Λ_{NMR}) is higher than that of the experimental molar conductivity value (Λ_{imp}) in the whole temperature range, which is analogous to the observation of other RTILs.[28, 29]

Discussion

Effects of Alkyl Chain Length on Ionic Diffusion. The microscopic ionic self-diffusion coefficient for the RTILs in this study contrasts with the macroscopically obtained viscosity, which resembles the behavior of other ionic liquids.[28,29] In general, the diffusivity is correlated to the fluidity ($1/\eta$) by the Stokes−Einstein equation

$$D = \frac{kT}{c\pi\eta r_s} \quad (6)$$

where k is the Boltzmann constant, T is the absolute temperature, c is a constant, and r_s is the effective hydrodynamic (Stokes) radius. All of the [Rmim][$(CF_3SO_2)_2$N] ionic liquids give approximately straight lines passing through the origin for change in the self-diffusion coefficients with $T\eta^{-1}$ (data not shown, $R^2 > 0.99$), indicating that eq 6 holds for the ionic diffusivity in the ionic liquids. It has been reported that from the results of the studies based on time-resolved emission spectra of probe molecules in RTILs, the solvation dynamics in the RTILs occurs on two distinct time scales.[31−33] The faster and slower ones are in ranges of $10^{-12}-10^{-10}$ and $10^{-10}-10^{-8}$ s, respectively.[31−33] The slower dynamics is linked to probe rotation time and solvent viscosity, which has been presumed to involve large-scale rearrangements of the RTILs.[31,32] Thus, the macroscopic viscosity seems to be reflected by the microscopic ion dynamics.

The factor c in the case of a large solute in a small solvent can attain the value of 6. If the ratio of the solute size to solvent is increased, especially for highly viscous media, the correlation breaks down, and the value of c in eq 6 is reduced to ca. 4.[34] The reported van der Waals radius from MM2 and ab initio molecular orbital calculations for [mmim], [emim], [bmim], [C$_6$mim], [C$_8$mim], and [$(CF_3SO_2)_2$N] is 0.287, 0.303, 0.330, 0.353, 0.373, and 0.326 nm, respectively.[35,36] By using the experimental slopes and the van der Waals radius, the factor c for the cationic diffusivity of [Rmim][$(CF_3SO_2)_2$N] with [mmim], [emim], [bmim], [C$_6$mim], and [C$_8$mim] can be obtained as 3.0, 2.9, 3.4, 3.4, and 3.6, respectively. Similarly, the c values for the anionic diffusivity are 4.4, 4.3, 4.3, 4.1, and 4.2 for [mmim], [emim], [bmim], [C$_6$mim], and [C$_8$mim], respectively. When the van der Waals radii are similar, the smaller c values of the cation than those of the anion suggest that the anion in the ionic liquids diffuses slower than the cation.

Figure 6 shows the apparent cationic transference number ($D_{cation}/(D_{cation}+D_{anion})$) for the RTILs as a function of temperature. The difference in the temperature dependency for the cationic transference number is apparent for the RTILs with change in the alkyl chain length. For the ionic liquids with relatively shorter hydrocarbon chains, the transference number decreases almost linearly with increasing temperature. This indicates relatively higher thermal acceleration of the [$(CF_3SO_2)_2$N] diffusion compared to the cationic diffusion, as was observed for other RTILs.[28,29] This is supported by the larger B values, in other words, larger activation energies for the diffusivity of the anions than those for the cations (Table 3) for the individual ionic liquids. As the alkyl chain length increases, the temperature dependency gradually becomes insignificant,

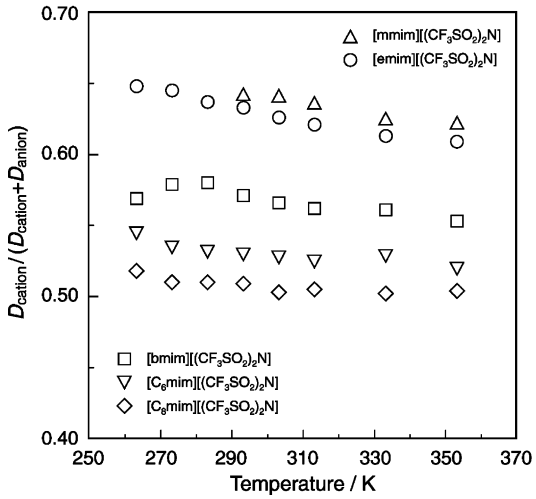

Figure 6. Apparent cationic transference number, ($D_{cation}/(D_{cation} + D_{anion})$), for [Rmim][$(CF_3SO_2)_2N$] ionic liquids plotted against temperature.

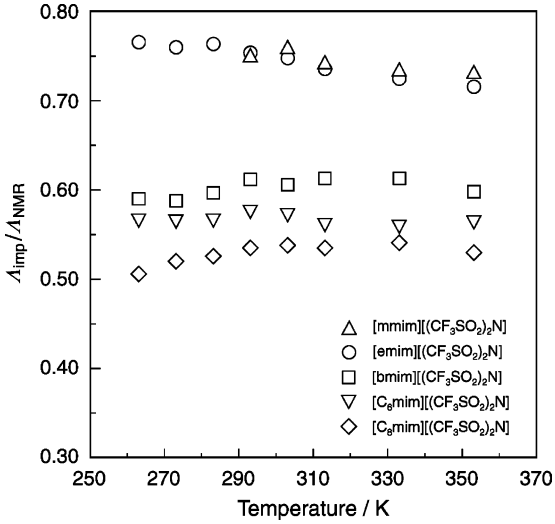

Figure 7. Molar conductivity ratios ($\Lambda_{imp}/\Lambda_{NMR}$) for [Rmim][$(CF_3SO_2)_2N$] ionic liquids plotted against temperature.

and for [C_8mim][$(CF_3SO_2)_2N$], no remarkable temperature dependency could be observed.

Despite a large disparity of the cationic and anionic radii, the transference number of [C_8mim][$(CF_3SO_2)_2N$] is estimated to be higher than 0.5. This indicates that the cation can diffuse faster than the anion, even if the cationic radius is larger than that of the anion. This is identical with the behavior of the [bmim]-based RTILs with different anionic structures and [$(CF_3SO_2)_2N$] liquids with different cationic structures.[29] The transference number decreases with increasing number of carbon atoms in the alkyl chain and is likely to be influenced by the size of the cation. However, [$(CF_3SO_2)_2N$] based ionic liquids with different cationic structures of similar cationic size show that the transference number is likely to be dominated by the ionic shape rather than the size.[29b] Thus, the relative diffusivity of the cation and anion of the RTILs in this study seems to be determined by both of the factors: ionic size and shape, and the relatively high cationic transference number of imidazolium-based ionic liquids up to 0.65 might come from the planar structure of the cationic backbone.

Karmaker and Samanta proposed that the biphasic (two distinct time scales) solvation dynamics in the RTMSs came from a relatively fast initial response of the anion and a slow collective diffusion of the cations and anions.[31] This consideration is based on smaller sizes of the anions. However, our results might imply that the fast motion of the cations was responsible for the biphasic solvation dynamics.

Ionic Association and the Interactive Forces Dominating the Properties of the RTILs. The ^{1}H and the ^{19}F NMR signals for the cation and anion always exhibit single lines without any multiplicity for each assigned nucleus, indicating that, even if there are dissociated, paired, and/or aggregated ionic species, the rate of exchange for the chemical equilibrium between the dissociated and associated ions in the ionic liquids is faster than the time scale of NMR measurements. The ion association and/or clusters could be observed in the FAB-MS measurements of the RTILs. For instance, the mass-to-charge ratio, $m/z = 111$ and 502, in the positive FAB mass spectrum for [emim][$(CF_3SO_2)_2N$] can be assigned to the quasi-molecular ion peaks of [emim] and [emim]$_2$[$(CF_3SO_2)_2N$], respectively. The $m/z = 280$, 699, and 1116 in the negative FAB spectrum for [emim][$(CF_3SO_2)_2N$] correspond to [$(CF_3SO_2)_2N$], [emim][$(CF_3SO_2)_2N]_2$, and [emim]$_2$[$(CF_3SO_2)_2N]_3$, respectively. Formation of such ion aggregates and/or clusters could also be observed in the FAB-MS results for all of the ionic liquids. The ionic association behavior, thereby, appears to be a common feature of RTILs.[29]

It is crucial to have an insight in the physicochemical processes in such RTILs based on the ionic association in the ionic liquids. The molar conductivity ratio, $\Lambda_{imp}/\Lambda_{NMR}$, which compares the molar conductivity obtained from the impedance measurement (Λ_{imp}) with that calculated from the ionic diffusivity (Λ_{NMR}), is introduced to quantify ionic association/dissociation under equilibrium in the RTILs. In fact, the $\Lambda_{imp}/\Lambda_{NMR}$ serves as an indicator of the percentages of ions contributing to the ionic conduction within the diffusing component. Since the term "degree of dissociation" is applied to dilute electrolyte solutions, the $\Lambda_{imp}/\Lambda_{NMR}$ may be defined as "ionicity" for ionic liquids, which are intrinsically extremely concentrated electrolytes. The molar conductivity ratio ($\Lambda_{imp}/\Lambda_{NMR}$) for the RTILs plotted against temperature is found to be relatively insensitive to the temperature (Figure 7). All of the RTILs give $\Lambda_{imp}/\Lambda_{NMR}$ values lower than unity, which indicates that only a part of the diffusive species in the ionic liquids contributes to the ionic conduction due to the presence of ionic association to generate nonconductive species in the system. The $\Lambda_{imp}/\Lambda_{NMR}$ value of the [Rmim][$(CF_3SO_2)_2N$] ionic liquids decreases with increasing number of carbon atoms in the alkyl chain. The addition of a $-CH_2-$ unit to the cation causes a decrease in the molar concentration (Table 2), which decreases the electrostatic attraction between the cation and anion. On the other hand, the increase in hydrocarbon units enhances the van der Waals interactions by means of the alkyl chains−ion inductive forces (dielectric polarization) and the hydrocarbon−hydrocarbon interactions, where the former inductive forces seem to be predominant in the RTILs.[37] The balance between these two opposite factors determines the ionic character of the system. The $\Lambda_{imp}/\Lambda_{NMR}$ values of the RTILs (Figure 7) indicate a significantly large contribution from the intermolecular inductive forces compared to the electrostatic attractions.[37]

Figure 8 depicts the change in the physical properties at 30 °C: viscosity, summation of cationic and anionic self-diffusion coefficients, molar conductivity, and $\Lambda_{imp}/\Lambda_{NMR}$, with change in the number of carbon atoms in the alkyl chain. With an increase in the number of carbon atoms, viscosity initially decreases from [mmim] to a minimum at [emim] and then increases with further increase in the alkyl chain length. This contrasts with the behavior of the summation of ionic self-

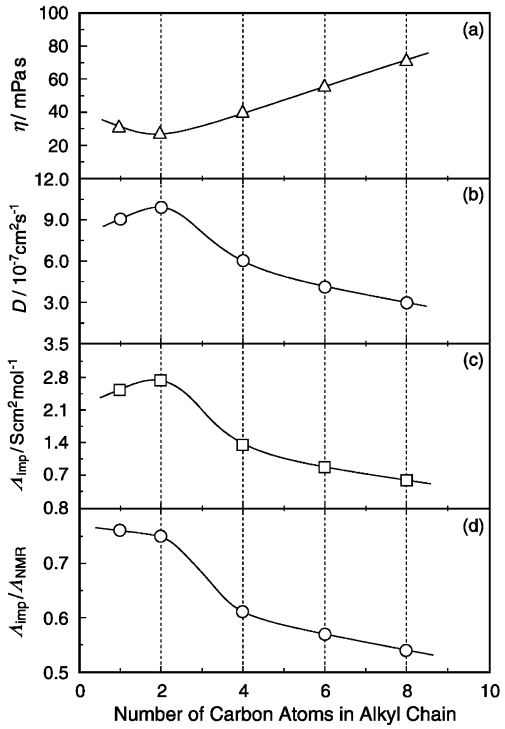

Figure 8. Alkyl-chain-length dependence of (a) viscosity, (b) simple summation of cationic and anionic self-diffusion coefficients, (c) molar conductivity from ionic conductivity and molar concentration, and (d) molar conductivity ratio ($\Lambda_{imp}/\Lambda_{NMR}$) for [Rmim][$(CF_3SO_2)_2$N] ionic liquids at 30 °C.

diffusion coefficients (Figure 8b) and molar conductivity (Figure 8c), which give similar profiles for changes with the alkyl chain length. However, the change in $\Lambda_{imp}/\Lambda_{NMR}$ with the number of carbon atoms in the alkyl chain shows somewhat different behavior (Figure 8d). The $\Lambda_{imp}/\Lambda_{NMR}$ values range from 0.54 to 0.76, while the summation of the ionic diffusion coefficients has values in the range from 3.0×10^{-7} to 9.9×10^{-7} cm^2 s^{-1}. The larger difference in the ionic diffusion coefficient, compared to that of the $\Lambda_{imp}/\Lambda_{NMR}$, indicates that the diffusivity is likely to cause significant changes in the molar conductivity (Λ_{imp}).

The high electrostatic interactions between the ionic species give the characteristic physicochemical properties of the ionic liquids and distinguish them from common organic solvents. However, the van der Waals (inductive) forces, as described above, also play an important role. For instance, with increasing number of carbon atoms in the alkyl chain, the inductive forces in the RTILs increase, which causes enhancement of the viscosity owing to frictional forces among ions, aggregates, and clusters. The cumulative effect of the ionic and the molecular characters of the RTILs has also recently been discussed by Angell and co-workers,[21] wherein they report that both the T_g value and the fragility are involved in determining the viscosity of given electrolyte salts including ionic liquids at ambient temperature. On the basis of the relation between the T_g and the molar volume of the salts with less polarizable anions, they evidenced a broad minimum in the ionic liquid cohesive energy at a certain intermolecular separation. The [Rmim][$(CF_3SO_2)_2$N] ionic liquids, therefore, provide a simplistic approach toward the understanding of the interactive forces, and change in the electrostatic and van der Waals forces with change in the number of carbon atoms in the alkyl chain can be visualized.

Concluding Remarks

The self-diffusion behavior of the RTILs with varying alkyl chain length of the imidazolium cation for a fixed anionic species, [$(CF_3SO_2)_2$N] in combination with our previous observations for other ionic liquids,[29] established the phenomenon of ion dynamics in the RTILs. The ionic diffusion coefficients obtained from PGSE-NMR methods greatly contrast with the viscosities, which clearly indicates that the microscopic ion dynamics reflects the macroscopic physical properties. In addition, the ionic diffusivity is significantly influenced not only by the ionic size, but also by the shape of the constituent ions. The ionicity, as quantified by the $\Lambda_{imp}/\Lambda_{NMR}$, has been proved to be a useful parameter to characterize significant properties of RTILs. The change in the alkyl chain length causes change in the interactive forces, and the properties of the RTILs are determined by the cumulative effect of the electrostatic interaction between the ionic species and the induction interactions between the ions, aggregates, and clusters. With the aim toward establishing a general aspect of the properties of the RTILs in terms of the interactive forces for variation in the structures, we would focus on such correlations and explore other common parameters affecting the physicochemical properties of RTILs in our future work.

Acknowledgment. This research was supported in part by Grant-in-Aid for Scientific Research (No. 14350452 and No. 16205024) from the MEXT. The authors acknowledge Mr. Takeo Kaneko (YNU) for the FAB-MS measurements and Dr. Seiji Tsuzuki (AIST) for discussion. H.T. and M.A.B.H.S. acknowledge JSPS, and K.H. acknowledges NEDO for financial support.

References and Notes

(1) *Ionic Liquids in Synthesis*; Wasserscheid, P., Welton, T., Eds.; Wiley-VCH: Weinheim, Germany, 2003.

(2) (a) Welton, T. *Chem. Rev.* **1999**, *99*, 2071−2083. (b) Holbrey, J. D.; Seddon, K. R. *Clean Prod. Process.* **1999**, *1*, 223−236. (c) Wassersheid, P.; Keim, W. *Angew. Chem., Int. Ed.* **2000**, *39*, 3772−3789.

(3) Bonhôte, P.; Dias, A.-P.; Papageorgiou, N.; Kalyanasundaram, K.; Grätzel, M. *Inorg. Chem.* **1996**, *35*, 1168−1178.

(4) (a) Holbrey, J. D.; Seddon, K. R. *Clean Prod. Process.* **1999**, *1*, 223−236. (b) Holbrey, J. D.; Seddon, K. R. *J. Chem. Soc., Dalton Trans.* **1999**, 2133−2139.

(5) (a) Sun, J.; MacFarlane, D. R.; Forsyth, M. *Ionics* **1997**, *3*, 356−362. (b) Sun, J.; Forsyth, M.; MacFarlane, D. R. *J. Phys. Chem. B* **1998**, *102*, 8858−8864. (c) MacFarlane, D. R.; Meakin, P.; Sun, J.; Amini, N.; Forsyth, M. *J. Phys. Chem. B* **1999**, *103*, 4164−4170.

(6) Mateus, N. M. M.; Branco, L. C.; Lourenço, N. M. T.; Afonso, C. A. M. *Green Chem.* **2003**, *5*, 347−352.

(7) Forsyth, S. A.; MacFarlane, D. R. *J. Mater. Chem.* **2003**, *13*, 2451−2456.

(8) (a) MacFarlane, D. R.; Forsyth, S. A.; Golding, J.; Deacon, G. B. *Green Chem.* **2002**, *4*, 444−448. (b) Pringle, J. M.; Golding, J.; Forsyth, C. M.; Deacon, G. B.; Forsyth, M.; MacFarlane, D. R. *J. Mater. Chem.* **2002**, *12*, 3457−3480.

(9) Golding, J.; Forsyth, S.; MacFarlane, D. R.; Forsyth, M.; Deacon, G. B. *Green Chem.* **2002**, *4*, 223−229.

(10) Yoshida, Y.; Muroi, K.; Otsuka, A.; Saito, G.; Takahashi, M.; Yoko, T. *Inorg. Chem.* **2004**, *43*, 1458−1462.

(11) (a) Matsumoto, H.; Yanagida, M.; Tanimoto, K.; Nomura, M.; Kitagawa, Y.; Miyazaki, Y. *Chem. Lett.* **2000**, 922−923. (b) Matsumoto, H.; Matsuda, T.; Miyazaki, Y. *Chem. Lett.* **2000**, 1430−1431. (c) Matsumoto, H.; Kageyama, H.; Miyazaki, Y. *Chem. Lett.* **2001**, 182−183.

(12) (a) Zhou, Z.-B.; Takeda, M.; Ue, M. *J. Fluorine Chem.* **2004**, *125*, 471−476. (b) Zhou, Z.-B.; Matsumoto, M.; Tatsumi, K. *Chem. Lett.* **2004**, 680−681. (c) Zhou, Z.-B.; Matsumoto, M.; Tatsumi, K. *Chem. Lett.* **2004**, 886−887.

(13) Larsen, A. S.; Holbrey, J. D.; Tham, F. S.; Reed. C. A. *J. Am. Chem. Soc.* **2000**, *122*, 7264−7272.

(14) (a) Hirao, M.; Sugimoto, H.; Ohno, H. *J. Electrochem. Soc.* **2000**, *147*, 4168−4172. (b) Yoshizawa, M.; Ogihara, W.; Ohno, H. *Electrochem. Solid State Lett.* **2001**, *4*, E25−E27.

(15) (a) Hagiwara, R.; Hirashige, T.; Tsuda, T.; Ito, Y. *J. Fluorine Chem.* **1999**, *99*, 1−3. (b) Hagiwara, R.; Hirashige, T.; Tsuda, T.; Ito, Y. *J. Electrochem. Soc.* **2002**, *149*, D1−D6. (c) Hagiwara, R.; Matsumoto, K.; Nakamori, Y.; Tsuda, T.; Ito, Y.; Matsumoto, H.; Momota, K. *J. Electrochem. Soc.* **2003**, *150*, D195−D199.

(16) Hagiwara, R.; Ito, Y. *J. Fluorine Chem.* **2000**, *105*, 221−227.

(17) (a) Koch, V. R.; Dominey, L. A.; Nanjundiah, C.; Ondrechen, J. *J. Electrochem. Soc.* **1996**, *143*, 798−803. (b) Nanjundiah, C.; McDevitt, S. F.; Koch, V. R. *J. Electrochem. Soc.* **1997**, *144*, 3392−3397. (c) MacEwen, A. B.; Ngo, H. L.; LeCompte, K.; Goldman, J. L. *J. Electrocehm. Soc.* **1999**, *146*, 1687−1695.

(18) Ngo, H. L.; LeCompte, K.; Hargen, L.; McEwen, A. B. *Thermochim. Acta* **2000**, *357*−*358*, 97−102.

(19) (a) Fox, D. M.; Awad, W. H.; Gilman, J. W.; Maupin, P. H.; DeLong, H. C.; Trulove, P. C. *Green Chem.* **2003**, *5*, 724−727. (b) Awad, W. H.; Gilman, J. W.; Nyden, M.; Harris, R. H.; Sutto, T. E.; Callahan, J.; Trulove, P. C.; DeLong, H. C.; Fox, D. M. *Thermochim. Acta* **2004**, *409*, 3−11.

(20) Huddleston, J. G.; Visser, A. E.; Reichart, W. M.; Willauer, H. D.; Broker, G. A.; Rogers, R. D. *Green Chem.* **2001**, *3*, 156−164.

(21) (a) Xu, W.; Cooper, E. I.; Angell, C. A. *J. Phys. Chem. B* **2003**, *107*, 6170−6178. (b) Xu, W.; Wang, L.-M.; Nieman, R. A.; Angell, C. A. *J. Phys. Chem. B* **2003**, *107*, 11749−11756

(22) (a) Cammarata, L.; Kazarian, S. G.; Salter, P. A.; Welton, T. *Phys. Chem. Chem. Phys.* **2001**, *3*, 5192−5200. (b) Seddon, K. R.; Stark, A.; Torres, M. J. *Pure Appl. Chem.* **2000**, *72*, 2275−2287.

(23) (a) Armstrong, D. W.; He, L.; Liu, Y.-S. *Anal. Chem.* **1999**, *71*, 3873−3876. (b) Anthony, J. L.; Maginn, E. J.; Brennecke, J. F. *J. Phys. Chem. B* **2001**, *105*, 10942−10949. (c) Blanchard, L. A.; Gu, Z.; Brennecke, J. F. *J. Phys. Chem. B* **2001**, *105*, 2437−2444.

(24) Lancaster, N. L.; Salter, P. A.; Welton, T.; Young, G. B. *J. Org. Chem.* **2002**, *67*, 8855−8861.

(25) Thomazeau, C.; Oliver-Bourbigou, H.; Magna, L.; Luts, S.; Gilbert, B. *J. Am. Chem. Soc.* **2003**, *125*, 5264−5265.

(26) (a) Carmichael, A. J.; Seddon, K. R. *J. Phys. Org. Chem.* **2000**, *13*, 591−595. (b) Aki, S. N. V. K.; Brennecke, J. F.; Samanta, A. *Chem. Commun.* **2001**, 413−414. (c) Muldoon, M. J.; Gordon, C. M.; Dunkin, I. R. *J. Chem. Soc., Perkin Trans. 2* **2001**, 433−435. (d) Crowhurst, L.; Mawdsley, P. R.; Arlandis, J. M. P.; Salter, P. A.; Welton, T. *Phys. Chem. Chem. Phys.* **2003**, *5*, 2790−2794.

(27) Baker, S. N.; Baker, G. A.; Kane, M. A.; Bright, F. V. *J. Phys. Chem. B* **2001**, *105*, 9663−9668.

(28) Noda, A.; Hayamizu, K.; Watanabe, M. *J. Phys. Chem. B* **2001**, *105*, 4603−4610.

(29) (a) Tokuda, H.; Hayamizu, K.; Ishii, K.; Susan, M. A. B. H.; Watanabe, M. *J. Phys. Chem. B* **2004**, *108*, 16593−16600. (b) Tokuda, H.; Ishii, K.; Susan, M. A. B. H.; Tsuzuki, S.; Hayamizu, K.; Watanabe, M. In preparation.

(30) (a) Vogel, H. *Phys. Z.* **1921**, *22*, 645−646. (b) Fulcher, G. S. *J. Am. Ceram. Soc.* **1923**, *8*, 339−355. (c) Tamman, G.; Hesse, W. *Z. Anorg. Allg. Chem.* **1926**, *156*, 245−257.

(31) (a) Karmakar, R.; Samanta, A. *J. Phys. Chem. A* **2002**, *106*, 4447−4452. (b) Karmakar, R.; Samanta, A. *J. Phys. Chem. A* **2002**, *106*, 6670−6675.

(32) Ingram, J. A.; Moog, R. S.; Ito, N.; Biswas, R.; Maroncelli, M. *J. Phys. Chem. B* **2003**, *107*, 5926−5932.

(33) Baker, S. N.; Baker, G. A.; Munson, C. A.; Chen, F.; Bukowski, E. J.; Cartwright, A. N.; Bright, F. V. *Ind. Eng. Chem. Res.* **2003**, *42*, 6457−6463.

(34) Cussler, E. L. *Diffusion: Mass Transfer in Fluid System*; Cambridge University Press: Cambridge, UK, 1984.

(35) (a) Ue, M. *J. Electrochem. Soc.* **1994**, *141*, 3336−3342. (b) Ue, M.; Murakami, A.; Nakamura, S. *J. Electrochem. Soc.* **2002**, *149*, A1385−A1388.

(36) The van der Waals radius of [mmim], [bmim], [C_6mim], and [C_8mim] was not available in the literature. However, cationic radii of some ionic liquids based on imidazolium, pyridinium, pyrrolidinium, and ammonium cation have been reported.[35b] Therefore, the radius of the imidazolium cations may be approximated by considering the radius of [emim] (0.303 nm) and that an increase in the alkyl chain length ($-CH_2-$) of the substituent of the tetraalkylammonium cation brings about an increase of about 0.160 nm.

(37) The attractive forces in the RTILs are mainly dominated by electrostatic and inductive forces due to less contribution of dispersion forces. The details of the simulating results for interactive forces will be discussed in our future publication.